STATIC AND DYNAMIC BEHAVIOR OF LENS-TYPE SHEAR PANEL DAMPERS FOR HIGHWAY BRIDGE BEARING

Tatsumasa Takaku, Feng Chen*,

Takashi Harada, Masayuki Ishiyama, Nobuhiro Yamazaki,**

Tetsuhiko Aoki*, and Yuhshi Fukumoto****

* Toko Engineering Consultants, Ltd., Tokyo, Japan. e-mails: takakus@tokoc.co.jp
** Nippon Chuzo Co., Ltd, Kawasaki, Japan. e-mail: n_yamazaki@nipponchuzo.co.jp,
*** Aichi Institute of Technology, Toyota, Japan. e-mail: aoki@aitech.ac.jp
**** Osaka University, Osaka, Japan. e-mail: yushi@mx3.mesh.ne.jp

Keywords: Shear Panel Damper, Low-yield Steel, Seismic Design, Dynamic Test, Bridge Bearing

Abstract. This paper describes a lens-type shear panel damper newly developed for highway bridge bearing. It has the form of concave lens shape made of low-yield steel LY 100. Both low yield strength and high ductility are the major requirements for damping devices. Response by static and dynamic shear tests results in rectangular shape of load-displacement hysteretic loops with high quality damping. Failure at the ultimate state highly depends on the cumulative deformation capacity of panel. Damage and life cycles can be estimated by Miner's rule. The analytical estimates agree well with the test findings. Large deformation of steel with high speed strain rate generates a lot of heat leading to high temperature of 300~400 ℃ on surface. Earthquake energy is converted to both strain and heat energies which results in large energy dissipation.

1 INTRODUCTION

The writers have investigated the performance of shear panel dampers made of low-yield steel LY 100 for bridge bearings, and static and dynamic tests have been conducted on a half size model of prototype to examine the fundamental properties of the damper [1]-[3]. This paper includes a seismic design methodology for the lens-type shear damper under several seismic excitations of Level 2 earthquakes specified in the code [4]. Random loading tests have been conducted to evaluate the structural and functional performance of the damper under the design level earthquakes and to determine the safety margin against collapse under exceedingly big earthquakes. For fracture evaluation, two types of prediction analysis, damage index method and damage pass method, are proposed.

2 DAMPERS, SPECIMENS AND TEST SETUP

2.1 Lens-type shear panel damper and half size model (Fig. 1)

Fig. 1 illustrates the panel details of a half size model of prototype for test use. In general, a damper system is composed of several components and the failure mechanism is rather complicated. The proposed shear panel consists of a single plate element only, and the failure mode is limited inside of the panel. In order to get a better damping performance, the panel details are modified according to the test results.
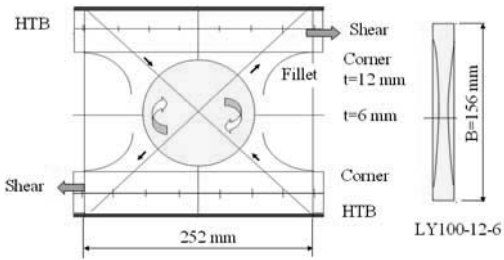
Fig. 1: Lens- type shear panel damper:
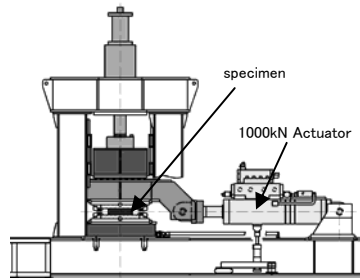Panel shape and connection

Fig. 2: Test setup

2.2 Specimens and test setup (Fig. 2, Table 1, and Table 2)

Measured and nominal properties of the low-yield steel of JFE-LY100 are listed in Tables 1 and 2. Test setup is shown in Fig. 2. Cyclic lateral load is applied to the upper setup beam. The max. capacity of an actuator is 250 mm in stroke, 1200mm/s in velocity and 1000KN in load. Friction type HTB and a shear key with small clearance of 0.5mm between sole plates, allowing small rotation, are used to connect the lower and upper setup beams.

Table 1 Measured mechanical properties of LY100-12-6

Yield stress(0.2%strain) σy	80 N/mm2
yield displacement(shear strain 3.2%) δy	5 mm
yield shear stress $\tau y = \sigma y / \sqrt{3}$	46.2 N/mm2
yield strenght Qy (at lens center,t=6mm)	66.1 KN
yield strenght Qy (at panel edge,t=12mm)	86.5 KN
Max.shear Qmax (at base with fillet)	245 KN
Qmax/Qy	2.80～2.87
δmax/δy	8～10
δ max	40～50 mm

Table 2 Mechanical properties of low yield steel (JFE LY100, nominal) LY100-12-6

Steel grade	LY-100
Yield strength	80～120 N/mm^2
Tensile strength	200～300 N/mm^2
Yield ratio	<60%
Elongation	>50%
Charpy value (at 0℃)	>27 J
Panel size、B/t	156x156x12mm,13
Concave lens (diameter, t)	130mm、t=6～12mm
Fillets	R=4t=48mm

3   STATIC AND DYNAMIC LOADING TESTS

3.1 Static tests: Gradually increased loading (δy to 10δy, shear strain 3.2% to 32%, and Table 4)

The increment of shear displacement in each cycle was ±δy, where δy=5mm was the shear yield displacement corresponding to the 0.2% offset yield shear stress of LY100 (Table 1).The displacement cycles were imposed until collapse at the final stage. One cycle was equivalent to shear strain of 3.2%. In the static loading tests, 10δy which was equivalent to the shear strain of 32% were recorded at the final stage, where severe cracking damage with large out-of plane twisted deformation was observed. The specimens left residual deformation after tests.

3.2 Sinusoidal loading tests: Harmonic motion of Sine wave with constant amplitudes.

Six kinds of amplitudes (5, 10, 20, 30, 35, and 40mm) and four kinds of velocity (slow and time periods of 0.5, 1.0, and 2.0 sec) were combined as test parameters. Slow speed was equivalent to static loading.

4 FUNDAMENTALS OF LENS-TYPE SHEAR PANEL: STATIC AND DYNAMIC TEST RESULTS

4.1 Lens behavior-1: Concave depth and failure modes (Fig. 3), "Lens makes for flexibility"

In general when the steel plate thickness increases, strength increases as well, but ductility reduces. Lens-type shear panel makes the best use of this property by changing the lens thickness and controlled failure modes. It is so designed to combine thicker edge around and thinner concave that allow low strength and high ductility with use of LY100. Failure modes highly depend on the concave depth. When the concave depth becomes deep, failure moves from the lens edge and fillet corners to the lens center where the cross sectional area becomes smallest in the panel. Fig. 3 shows the static test results for various lens shapes. In the static tests of LY100-12-8, LY100-12-6(Fig.2), and LY100-12-4, the maximum displacements count up to 8δy, 9δy, and 10δy in proportion to the concave deepness. On the contrary, LY100-12-3 shows different behavior. It collapsed at the edge around and center at the same time for the maximum displacement of 8δ y . Early crack initiation at the lens center due to the alternate tension field was observed. This phenomenon was clearly observed in the dynamic test. Taking safety margin into consideration, LY100-12-6 was recommended to be the best use for shear panel dampers.
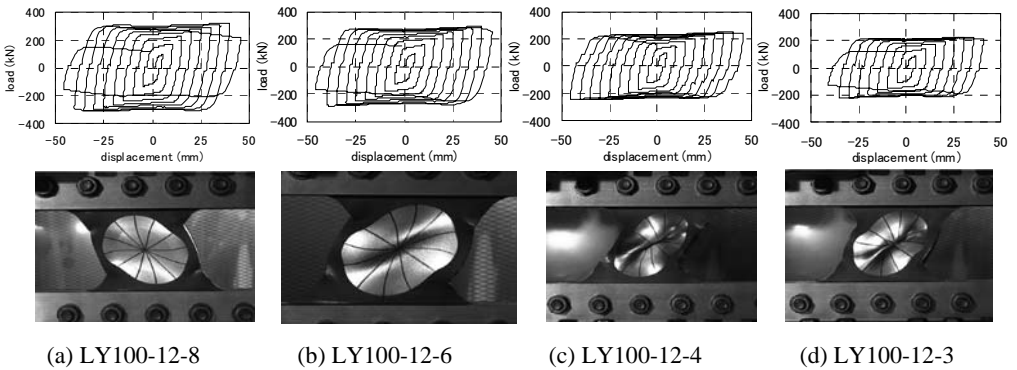
| (a) LY100-12-8 | (b) LY100-12-6 | (c) LY100-12-4 | (d) LY100-12-3 |

Fig. 3: Lens behavior-1: Concave depth and failure modes

4.2 Lens behavior-2: Fillets and failure modes (Fig. 4),"Too large fillet cut lens center"

(a) static test
(gradually increased test)

(b) dynamic test
(sinusoidal test ,amplitude 20mm)

Temp:337℃

Temp:242℃

(a) Lens panel

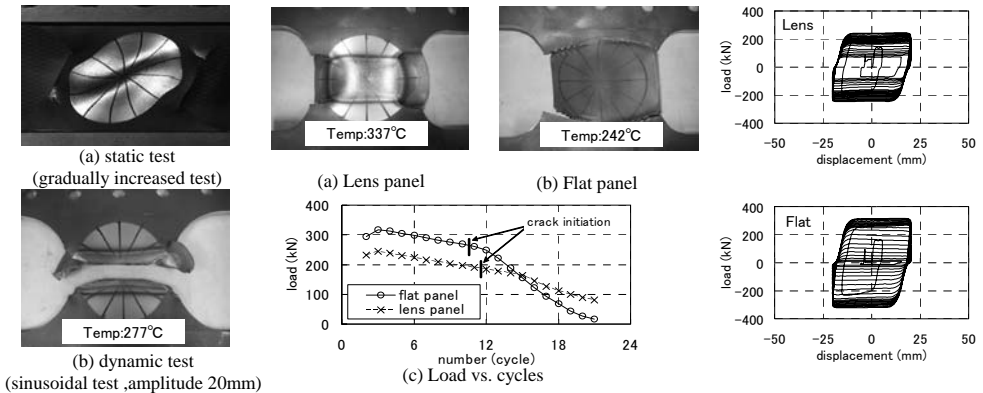(b) Flat panel

(c) Load vs. cycles

Lens

Flat

Fig. 4: Lens behavior-2: fillet and failure modes (R=6.5t=78mm)

Fig.5: Lens behavior-3: load versus loading cycles for lens and flat panels (Sinusoidal test for amplitude=20mm and T=1sec)

Fillet at the panel corner plays an important role to reduce the local stress concentration and consequently, to control the failure mode of cracking. When fillet is too large in size, cracking initiates

at the lens center. In design sense, it is preferable to fail at the four corners instead of lens center for better ductility. Fig. 4 shows for R=6.5t case. In the static tests, peak shears for R=4t and R=6.5t are 291KN and 330KN, respectively where cracks initiate at the same panel corners. In the dynamic test, both cases show different failure modes. In the case of R=4t, cracks stay at the corners. While, for R=6.5t cracks initiate at the center. In the case of R=4t (Fig.5(a)), wider plastic zone and higher temperature up(377℃) are recognized than for R=6.5t, which means the panel for R=4t has better ductility.

4.3 Lens behavior-3: Lens panel and flat panel (Fig. 5),"Flat panel is fragile in dynamics"

Fig. 5 shows the dynamic test results; failure modes of LY100-12-6 (lens) and LY100-12-12 (flat) for the constant amplitude of ±20mm.In the static test, both show similar failure mode. In proportion to the cross sectional area, the shear force recorded 245KN and 315KN, respectively. In contrast to the static test, the dynamic test results provided different type of behavior definitely. In the case of LY100-12-6, the plastic zones accompanied with heat radiation spread out widely in the radial direction from center to outside, with high temperature of 337℃ on the surface. In the case of LY100-12-12, the plastic zone is limited to a narrow band with less temperature of 242℃. Fig. 5 shows the load versus repeated cycle. After 12 cycles, significant crack damage at the edges causes sudden drops of deterioration. Passage of crack propagation left irregularity like gear notch.
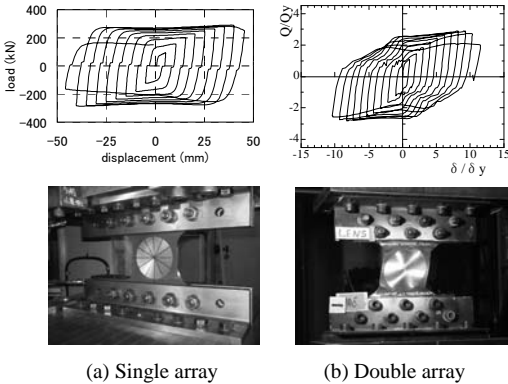

(a) Single array   (b) Double array

Fig. 6: Panel connection: Use HTB (friction type)

Fig. 8: Cumulative displacement capacity versus wave amplitude

4.4 Panel connections: Use friction type HTB (Fig. 6),"Boundary changes ductility"

Major requirements for specimen connections are as follows:

1.   It should transfer seismic lateral forces to shear panel damper tightly with strong enough rigidity so that damping effect is performed completely.

2.   Panel edges should be so tightly fixed that it resists both against moment and shear. It is recommended to set double array HTB rather than single arrangement. Single array HTB allows slight rotation due to moment which results in semi-rigid connection.

3.   At the ultimate state of failure, the cracking in the tension state is more critical than buckling in compression. Friction type HTB is available to reduce the stress concentration with less local constraints. Large deformation causes big thickness changes in the 3-dimensional directions so that it causes cracking at the constraint points such as welding deposits.

Fig. 6 shows the panel behavior connected by single (Case A) and double (Case B) array HTB. In Cases A and B, $Q_{max}/Q_y=2.8\sim2.87$ and $2.8\sim2.90$, and $\delta_{max}/\delta_y=9$ and 10, respectively. Note that the boundary changes both strength and ductility. Since the specimen size is limited to small due to the
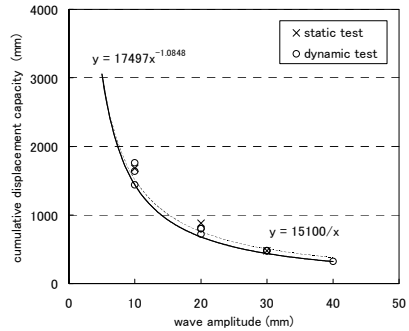
available capacity of loading frame and actuator, a half size model with single array HTB, Case B, was tested at the Aichi Institute of Technology.

4.5 Analytical model: Bilinear model with rectangular shape by static and dynamic tests (Fig. 7)

Fig. 7 shows the typical load-displacement hysteretic curves for 30mm constant amplitude under the sinusoidal tests (two cases of slow and T=1sec).The peak load gradually decreases with cycles and the cracking starts at 6 cycles. Fig. 7 also shows an assumed analytical model, a bilinear model of rectangular shape, where two parameters of Qmax and S1 are defined. The maximum loads, Qmax and Qpeak are determined; Qmax for analytical model denotes the average value of resistance shears, and Qpeak for design use is the highest value among them. Qpeak /Qmax is about 1.13～1.18, both in the static and dynamic tests. S1 is determined from the unloading gradients. The values of Qmax, Qpeak, Qpeak/Qmax and S1 are determined as 245K, 282KN, 1.15 and 140KN/mm, respectively.
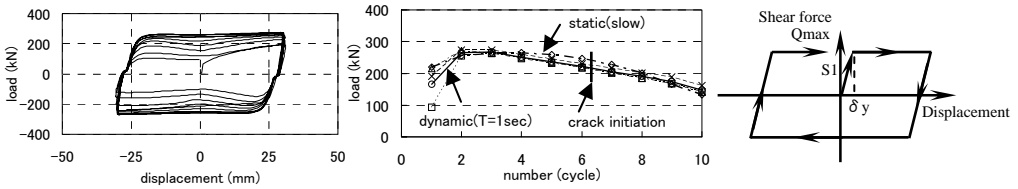
Sinusoidal test (sine wave, amplitude 30mm, slow and T=1sec)
Fig. 7: Analytical model: bilinear model with rectangular shape (Q_{max}, S1)

5   CUMULATIVE DISPLACEMENT CAPACITY (CDC) AND HEAT TRANSFER

5.1 Sinusoidal test results: CDC and damage index (Fig. 8 and Table 3)

Table 3 sine test results, cumulative displacement capacity and damage index $1/N_f$

amplitude	period	velocity	num.of cycles to failure	modified cf*	limit disp. (test results)	deformed capacity	critical disp. (Cdc)	num.of cycles to failure	damage index
x(mm)	T(sec)	v (mm/s)	C_f	d/4x	d(mm)	x*d(mm2)	y=15100/x	N_f=15100/4x^2	1/N_f
5	1	31	170	168	3360	16800	3020	151	0.0066
10	2	31	38	36	1440	14400	1510	37.8	0.0265
10	1	63	46	44	1760	17600	1510	37.8	0.0265
10	0.5	126	43	41	1640	16400	1510	37.8	0.0265
15	1	94	17	15	900	13500	1007	16.8	0.0596
20	2	63	12	10	800	16000	755	9.4	0.1060
20	1	126	12	10	800	16000	755	9.4	0.1060
20	0.5	251	11	9	720	14400	755	9.4	0.1060
30	2	94	6	4	480	14400	503	4.2	0.2384
30	1	188	6	4	480	14400	503	4.2	0.2384
30	0.5	377	6	4	480	14400	503	4.2	0.2384
40	1	251	4	2	320	12800	378	2.4	0.4238
Specified(averaged) values for design									
18.875	1			10.6	800	15100	800	10.6	0.094

The displacement capacity which has strong relation to the strain energy capacity depends greatly on the strain rate and seismic magnitude (EQ), the stress states and intensity (panel shape), and the fracture toughness (LY100).As a performance indicator, the cumulative displacement capacity Cdc is used for their evaluation.Table-3 summarizes the 12 case test results which deal with CDC and the number of cycles to failure N_f versus constant wave amplitude x (5, 10, 15, 20, 30, and 40 mm). The relationship between the cumulative displacement capacity (y and Cdc) to the wave amplitude (x) is shown in Fig. 8.

$$y = 17497 x^{-1.0848} \tag{1}$$

$$xy = 15100 \tag{2}$$

Eq.(1) is derived from the test data through regression analysis, and Eq.(2) is a simplified hyperbola of Eq.(1) showing x times y is equal to constant which characterizes lens identity. Based on Miner's rule，N_f and damage accumulated in each cycle D_f are given by Eqs.(3),and(4), respectively.

$$N_f = 15100/4x^2 \tag{3}$$

$$D_f = 1/N_f \tag{4}$$

Miner's rule gives the design criteria to failure by Eq. (5).

$$D_1 = \sum \left(1/N_f\right) < 1 \tag{5}$$

For example, in Table 3, when a damper is subjected to a harmonic motion with a specified amplitude x=18.875mm, its survival number of cycles N_f and the damage index D_f are 10.6 and 0.094, respectively.

By using the analytical data of traveled pass D_{tp}, the damage pass $D_{tp}*$ is defined by Eq.(6).

$$Dtp* = \sum \left(\text{damage pass coefficient e}\right) \cdot \left(\text{response amplitude x}\right) = \sum \left(4x^2/18.875\right) \tag{6}$$

where e=x/18.875and Cdc=800mm. Safety of D_2 can be evaluated by Eq.(7).

$$D_2 = \sum \left(Dtp^*/800\right) < 1 \tag{7}$$

CDC can be evaluated by the two methods: 1) Damage index method by Eq. (3), (4), and (5),and 2) Damage pass method by Eq.(6) and (7). Both results give the same answer exactly, because they stand on the same base of Eq.(2). Damage index method has an advantage to evaluate the damage state without determination of cumulative damage pass limit (Cdc). A trial simulation is shown in Table 4.

Table 4 Gradually increased displacement tests: cumulative displacement and design limit

loading	amplitude x(mm)	Trav. pass $\Sigma(4x)$	damage index method				damage pass method		
			$N_f=15100/4x^2$	$1/N_f$	$D_1=\Sigma(1/N_f)$	e=x/18.875	e* x	Q=$\Sigma(4e*x)$	D_2=Q/800
δy	5	20	151.0	0.007	0.007	0.265	1.32	5.3	0.007
$2\delta y$	10	60	37.8	0.026	0.033	0.530	5.30	26.5	0.033
$3\delta y$	15	120	16.8	0.060	0.093	0.795	11.92	74.2	0.093
$4\delta y$	20	200	9.4	0.106	0.199	1.060	21.19	158.9	0.199
$5\delta y$	25	300	6.0	0.166	0.364	1.325	33.11	291.4	0.364
$6\delta y$	30	420	4.2	0.238	0.603	1.589	47.68	482.1	0.603
$7\delta y$	35	560	3.1	0.325	0.927	1.854	64.90	741.7	0.927
$8\delta y$	40	720	2.4	0.424	1.351	2.119	84.77	1080.8	1.351
$9\delta y$	45	900	1.9	0.536	1.887	2.384	107.28	1509.9	1.887
design limit	35	900			$D_1<1$			800	$D_2<1$

5.2 Gradually increased displacement tests and evaluation of CDC: design criteria (Table 4)

Table 4 shows the test results for gradually increased displacement history and evaluation of CDC by damage index method and damage pass method. At 7δy, the cumulative damage $D_1=\Sigma(1/N_f)$ becomes 0.927, that is, the D_1 value is close to 1 indicating almost failure. In the static test, the max. displacement counts up to 9δy with traveled pass 900mm. In the dynamic test, the estimated max. displacement is reduced to 7δy, where the damaged traveled pass is 741mm, that is, a little below the cumulative displacement limit value of 800mm. Design criterion can be safely proposed that D_s (static max. displacement), D_d (dynamic max. displacement), $D_{tp}*$(damage pass), can be determined less than 45mm (9δ y), 35mm (7δy)， 800mm, respectively.

5.3 Energy Dissipation by heat transfer: "High speed strain rate generates heat"(Figs. 4, 5,and 9)

Large displacement with high speed strain rate generates heat in steel. However, mechanism of heat generation system of steel caused by high strain rate has not been solved yet theoretically in the study. Observations and comments are described as follows:

1. Heat was generated only in the dynamic test, not in the static test. Slight temperature up was observed in the dynamic random test.

2. Between time period of 0.5 and 2.0 sec., no remarkable difference of heat-up temperature was observed, keeping 300~400℃ on the panel surface.

3. Plastic zone and heat radiation spread out widely in the radial direction from lens center to outward.

4. Cracking delay was observed: It seems that expansion due to heat reduces the stress concentration. Heat transfer contributes to the energy dissipation, and consequently good ductility is expected.

5. In random loading, recorded temperature up is limited to 40~50℃,which means that the seismic behavior is close to the static one when subjected to actual earthquakes.

6 RANDOM LOADING AND TEST RESULTS: SAFTY MARGIN AND LIFE CYCLE

6.1 Random loading tests: Test program (EQ, amplification factor, and damper model)

A full scale bridge model and one-degree-of-freedom model with dampers are used for the dynamic analysis, and their responses are provided to the random loading test as displacement control data. Three types of Level 2 specified earthquakes (EQ2-2-1, EQ2-2-2, EQ2-2-3)[4] and their amplification factors (1.0 and 1.2) are combined as test parameters. As damper models, stiff (S) and regular(R) models with different stiffness are considered (Table 5).In total, 8 cases (E1~E8) are considered.

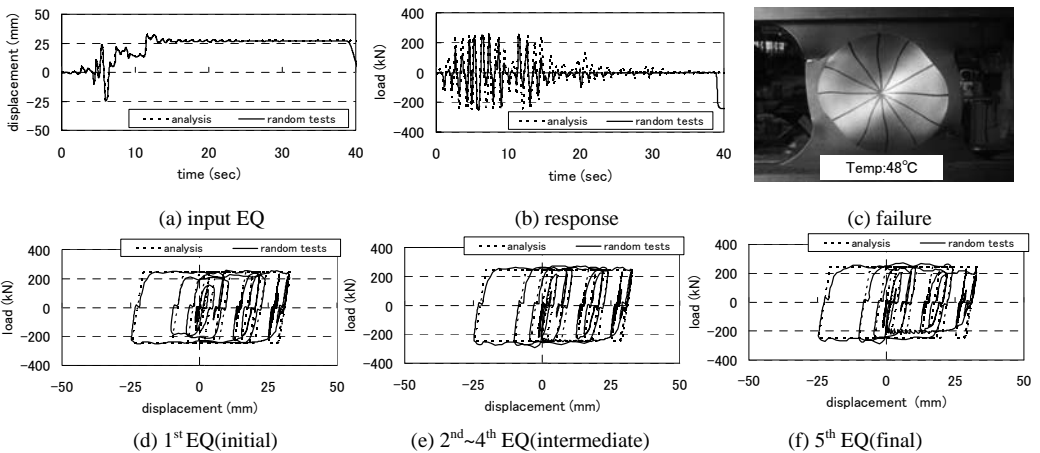## 6.2 Random test results: Comparison with analysis (Qmax and Qpeak) (Fig. 9 and Table 5)

(a) input EQ	(b) response	(c) failure
(d) 1st EQ(initial)	(e) 2nd~4th EQ(intermediate)	(f) 5th EQ(final)

Fig. 9 Repeated random loading test results for Level-2, EQ2-2-1,and s=1.2

Time-history of displacement and resistance (Q_{peak} and Q_{max})

Fig. 9 shows the test results which explain time-history of displacement and shear resistance of damper.

1. Displacement time-history: Loading is applied to the damper by the displacement control, and input to actuator should be equivalent to output records.

2. Resistance time-history for Q_{max} and Q_{peak}: Damper stiffness model is based on the hysteretic curves in the static tests, and analytical model assumed a rectangle shape shown in Fig. 7. In a half size model, Q_{max} and Q_{peak} are determined as 245KN and 282KN,Q_{peak}/Q_{max}=1.15, for damper S-model. Response time-history verifies that the damper shear resistance is always below Q_{peak} keeping in safe region.

6.3 Random test results: strength (safety margin) and endurance (life cycle)

Table 5 shows the test results for the repeated random loading. Combined 8 cases with Level 2 EQ (EQ2-2-1, EQ2-2-2, and EQ2-2-3) and amplification factors (1.0and1.2) are described. In each case, the tests result is compared with the prediction. In test, max./min. displacement and the number of cycles to failure, c1and c2, are counted, where c1and c2 are the observed cycles to crack initiation and to failure at the final state, respectively. Average (life) cycle cf=(c1+c2)/2 is used for comparison with the prediction. Both damage index and damage pass methods are used for the predicted data. The predicted N_f can explain well the test data of life cycles cf. As design criteria, it is proposed that the N_f value should be greater than 3, which means a damper can survive at least in three times of Level 2 earthquake. In fact, big earthquakes are always accompanied by aftershocks in a few days without repair time. Shear panels connected by HTB are so designed as to repair easily in a short time once damages are found.

Table-5 Random loading test results and comparison with failure prediction

Case	damper model	random loading level-2 EQ	ampl.factor s	test results: response and cf			prediction by Dtp* and N_f		
				cf	max.disp. (mm)	travel.pass (mm)	Dtp*	800/Dtp*	N_f
E1	R	EQ2-2-1	1	4.5	33.6	325.1	183	4.37	4.37
E2	R	EQ2-2-2	1	5.5	22.9	321.5	160	4.99	4.99
E3	R	EQ2-2-3	1	5.5	14.8	235.3	123.9	6.46	6.46
E4	R	EQ2-2-1	1.2	3	40.3	390.1	263.3	3.04	3.04
E5	R	EQ2-2-2	1.2	4.5	27.5	386	229.3	3.49	3.49
E6	R	EQ2-2-3	1.2	4.5	17.8	265.2	177.1	4.52	4.52
E7	S	EQ2-2-1	1.2	4.5	33.1	332.6	182.9	4.37	4.37
E8	S	EQ2-2-1	1	6	27.6	272.6	124.8	6.41	6.41
estimate1	S	EQ2-2-1	1.2		33.1	327.1	179.7	4.45	4.45
estimate2	S	EQ2-2-1	1.46		40.3	398.0	266.0	3.01	3.01

damper model: R(regular)model;Qmax=225KN,S1=134KN/mm,S(stiff)model ; Qmax=245KN,S1=140KN/mm,Dtp*:damage pass
s:amlification factor, estimate: scaled by a parameter (s)on the basis of E8(s=1)

6.4 Influence of amplification factor s to dynamic response: $D_{tp}*$ and N_f are scaled by s^2

Displacements and traveled pass are simply scaled by s. On the other hand, damage pass $D_{tp}*$ and N_f are scaled by s^2.Table-5 shows the estimated response values. N_f is easily estimated by the parameter s.

7   CONCLUSIONS

1. Shear panel damper is developed as a part of function-separated bearing system to serve for lateral seismic loads, and it provides easy maintenance and urgent repair works once being damaged.

2. As a shear panel, the concave lens shape +low-yield steel LY100 gives the most effective way to satisfy the requirements of low strength and high ductility with large energy dissipation.

3. Large deformation of low-yield steel with high speed strain rate provides new findings in this study: Two items are crucial needed for further study : 1) cumulative deformation capacity, and 2) energy dissipation by heat transfer.

REFERENCES

[1]   Aoki,T.,Liu,Y.,Takaku,T.,Uenoya,M.,&Fukumoto,Y.,2007. Experimental investigation of tapered shear type seismic devices for bridge bearings.*Proc.,8th Pacific Structural Steel Conference (PSSC)*,New Zealand, March 2007.1,111-117.

[2]   Aoki,T., Liu,Y.,Takaku,T.,&Fukumoto,Y.,2008.A new type of shear panel dampers for highway bridge bearings. *EUROSTEEL2008*, 3-5, September 2008, Graz, Austria.

[3]   Aoki,T., Dang.J., Zhang.C., Takaku,T.,& Fukumoto,Y., Dynamic shear tests of low-yield steel panel dampers for bridge bearing. *Proc., of 6th International Conference of STESSA* 2009,16-20 August 2009, Philadelphia, USA.

[4]   Japan Road Association: *Specification for Highway Bridges*, Part 5, Seismic Design 2000.